

# On the Use of the Geoid in Geophysics: A Case Study Over the North-West Shelf of Australia

**W. E. Featherstone**

*School of Surveying and Land Information*

*Curtin University of Technology*

*GPO Box U1987*

*Perth WA 6001*

email: Featherstone\_WE@cc.curtin.edu.au

## ABSTRACT

The geoid is the fundamental surface that defines the figure of the Earth. It is approximated by mean sea-level and undulates due to spatial variations in the Earth's gravity field. The use of the geoid in regional geophysics is illustrated for the North-West Shelf of Australia by removing long-wavelength geoid features, due predominantly to deep-Earth mass anomalies, in order to reveal near-surface structure. After this process, the residual geoid anomalies correlate well with known geological structures. Therefore, the geoid can provide information, complementary to other geophysical data, of the Earth's internal structure.

Key words: geoid, geodesy, tectonic elements, spectral analysis

## INTRODUCTION

The geoid can be described as *the equipotential surface of the Earth's gravity field which corresponds most closely with mean sea-level in the open oceans and ignores the effects of semi-dynamic sea surface topography*. It defines the figure of the Earth and is used as the vertical datum surface in most countries. The determination of the geoid has attracted much attention within the discipline of geodesy, where both theoretical and practical problems are studied in order to improve the definition and accuracy of the geoid. This has been possible since the publication of the famous (to geodesists) integral formula by George Gabriel Stokes in 1849. Early attempts were made to

compute the geoid between the 1930s and 1950s, but these were severely restricted by the availability of accurate terrestrial gravity data. Only after the launch of geodetic satellites in the late 1950s and early 1960s could global geoid determination begin in earnest. More recently, a precise determination of the geoid at a regional scale has been demanded in order to transform Global Positioning System (GPS)-derived heights to heights above mean sea-level. As such, the determination of the geoid has become a revived research area since the mid-1980s, and many geoid solutions are now available at both global and regional scales. Once determined, the geoid provides geopotential field information, whose form can be interpreted by the geophysicist in terms of the internal properties of the Earth (Chapman, 1979). Therefore, the geoid provides a valuable tool for both the geodesist and the geophysicist.

The use of the geoid in geophysics is the subject of a recent book, edited by Vanicek and Christou (1994), which discussed the relationships between the geoid and deep-Earth mass density anomaly structure, strain and stress fields, tectonic forces, the isostatic state of oceanic lithosphere, Earth rotation, geophysical prospecting, and ocean circulation. However, the importance of the geoid in geophysics had been recognised for some time before this (eg, Kaula, 1967; Chase, 1985; Lambeck, 1988), which is shown further by notable studies such as:

- correlation between the geoid and deep-Earth mass density anomalies (Bowin, 1983) and near-

surface mass density anomalies (Christou et al., 1989);

- correlation between the geoid and mantle convection (Runcorn, 1967), and the constraints provided by the geoid on mantle rheology and flow (Hager, 1984);
- correlation between the geoid and westward drift of the geomagnetic field (Khan, 1971); and
- correlation between the geoid and plate tectonic features and seismic tomography (Silver et al., 1988).

Despite these studies in global geophysics, the geoid has not gained such a level of acceptance by the geophysical exploration community, probably because of its perception as 'simply another set of gravity data'.

This paper presents the application of the geoid in geophysics as used by Featherstone (1992), where the geoid was shown to accurately map the position of geological features beneath the North Sea. It should be noted, however, that this discussion does not aim to promote the virtues of the geoid as a geophysical tool in its own right. Instead, the geoid simply provides a complementary source of information to the geophysicist. To illustrate this, a case study area has been chosen over the North-West Shelf of Australia, which has recently received the attention of petroleum geophysicists (eg, Purcell and Purcell, 1988; 1994). The hypothesis used is that geoidal undulations can be interpreted as being generated primarily by geologically well-known features beneath the North-West Shelf. This, by implication, will illustrate that the geoid has the capability of detecting previously unknown features in this and other regions of geophysical interest.

## DETERMINATION OF THE GEOID

The determination of the geoid has attracted the attention of many geodesists, and with the advent of GPS there is now an abundance of literature on its

definition and practical computation. Therefore, instead of simply duplicating this information, a summary is given, together with the citation of reference materials on the broader subject matter.

The position of the geoid with respect to a pre-defined reference surface, usually the mean-Earth ellipsoid, can be determined using either geometrical or physical methods. Modern geometrical techniques include GPS and satellite radar altimetry. On land, GPS measurements, when co-located with vertical benchmarks, give discrete measurements of the position of the geoid. However, these are generally sparse and thus do not provide information of use to the geophysicist. At sea, satellite radar altimetry can be used to give a direct measure of the ocean surface (eg, Shum et al., 1995), which is a close approximation (to within two metres) of the geoid. These satellite altimeter measurements of the geoid can also be used to derive the marine gravity field (eg, Sandwell and McAdoo, 1988).

The physical geodetic approach to geoid determination uses a combination of satellite-derived and terrestrial gravity observations to determine the gravimetric geoid, either over the whole Earth or over a particular region. The modern approach is based on Stokes's (1849) integral and the remove-restore technique, in which a global geopotential model is combined with surface gravity and terrain data. This approach dispenses with the need for global gravity data in the original Stokes formula. The specific details of the gravimetric determination of the geoid are given by, for example, Vanicek and Christou (1994).

### The Geoid of the North-West Shelf

To illustrate the use of the geoid in the North-West Shelf region of Australia, two existing gravimetric geoid solutions have been utilised. These are the OSU91A global geopotential model (Rapp et al., 1991) and the regional AUSGEOID93 geoid model (Steed

and Holtznagel, 1994). OSU91A was computed from a combination of data derived from the analysis of the orbits of artificial Earth satellites, terrestrial gravity and terrain data, and marine gravity data derived from satellite altimetry. This global model provides geoid and gravity information at a spatial resolution of approximately 55 km. On the Australian continent, the OSU91A model has been refined by the inclusion of terrestrial gravity data at a resolution of approximately 10 km to form the regional AUSGEOID93. However, AUSGEOID93 does not cover the North-West Shelf, which necessitates the use of the OSU91A geoid model offshore to illustrate the use of the geoid in this region.

If available, a regional geoid of the area of interest should be used in preference because differences of up to 10 m are known to exist between current global geopotential models (Rapp and Wang, 1993), which can adversely affect any subsequent geophysical interpretations. However, the OSU91A model has been shown to provide the most accurate fit of all recent geopotential models to the geoid and gravity field of Australia (Zhang and Featherstone, 1995). Therefore, it is reasonable to assume that this model also provides an accurate representation of the geoid over the North-West Shelf of Australia.

The geoid height above the reference ellipsoid ( $N$ ) is computed from the spherical harmonic coefficients that define the OSU91A global geopotential model (Rapp et al., 1991) by:

$$N = \frac{GM}{r\gamma} \sum_{n=2}^{M_{\max}} \left(\frac{a}{r}\right)^n \sum_{m=0}^n (C_{nm} \cos m\lambda + S_{nm} \sin m\lambda) P_{nm}(\cos \theta) \quad (1)$$

where  $GM$  is the geocentric gravitational constant;  $\gamma$  is normal gravity on the reference ellipsoid;  $(r, \theta, \lambda)$  are the spherical polar coordinates of the computation point;  $a$  is the equatorial radius;  $P_{nm}(\cos \theta)$  are the fully normalised associated Legendre functions for degree  $n$  and order  $m$ ; and  $\delta C_{nm}$  and  $S_{nm}$  are the fully normalised OSU91A coefficients, reduced for the even

zonal harmonics of the ellipsoid, and complete to degree and order  $M_{\max} = 360$ .

The corresponding free-air gravity anomalies ( $\Delta g$ ) can be computed from the OSU91A coefficients by first inserting equation (1) into the spectral relation given by Heiskanen and Moritz (1967, p. 97)

$$\Delta g_n = \frac{\gamma(n-1)}{r} N_n \quad (2)$$

This relation shows that the determination of the geoid from free-air gravity anomalies is essentially a shift of power in the geopotential spectrum. The free-air gravity anomalies are thus determined from the OSU91A global geopotential model by:

$$\Delta g = \frac{GM}{r^2} \sum_{n=2}^{M_{\max}} \left(\frac{a}{r}\right)^n (n-1) \sum_{m=0}^n P_{nm}(\cos \theta) \times \dots (C_{nm} \cos m\lambda + S_{nm} \sin m\lambda) \quad (3)$$

The OSU91A geopotential coefficients are freely and widely available, and the computations described herein have used a modified version of Rapp's (1982) algorithms. The degree  $M_{\max} = 360$  expansion of OSU91A has been evaluated for the North-West Shelf region of Australia between latitudes 10°S and 24°S and longitudes 110°E and 132°E. This has been supplemented by the AUSGEOID93 geoid model on land to produce the geoid shown in Figure 1.

The geoid map of the North-west Shelf in Figure 1 evidently contains some high resolution information, which is closely correlated with the known structural elements summarised in Australian Geological Survey Organisation North-West Shelf Study Group (1994). However, the geoid in this region is dominated by a long wavelength, south-west to north-east trend. The geoid height relative to the reference ellipsoid varies from -33 m in the south-west up to +59 m in the north-east. This variation corresponds to a geoidal gradient of approximately 32 mm/km (ppm), which obscures a large amount of the geophysically more

interesting short-wavelength information. Obviously, this trend is of hindrance to any geophysical interpretation of the geoid on a regional scale and

must therefore be removed in order to reveal the short-wavelength details more clearly.

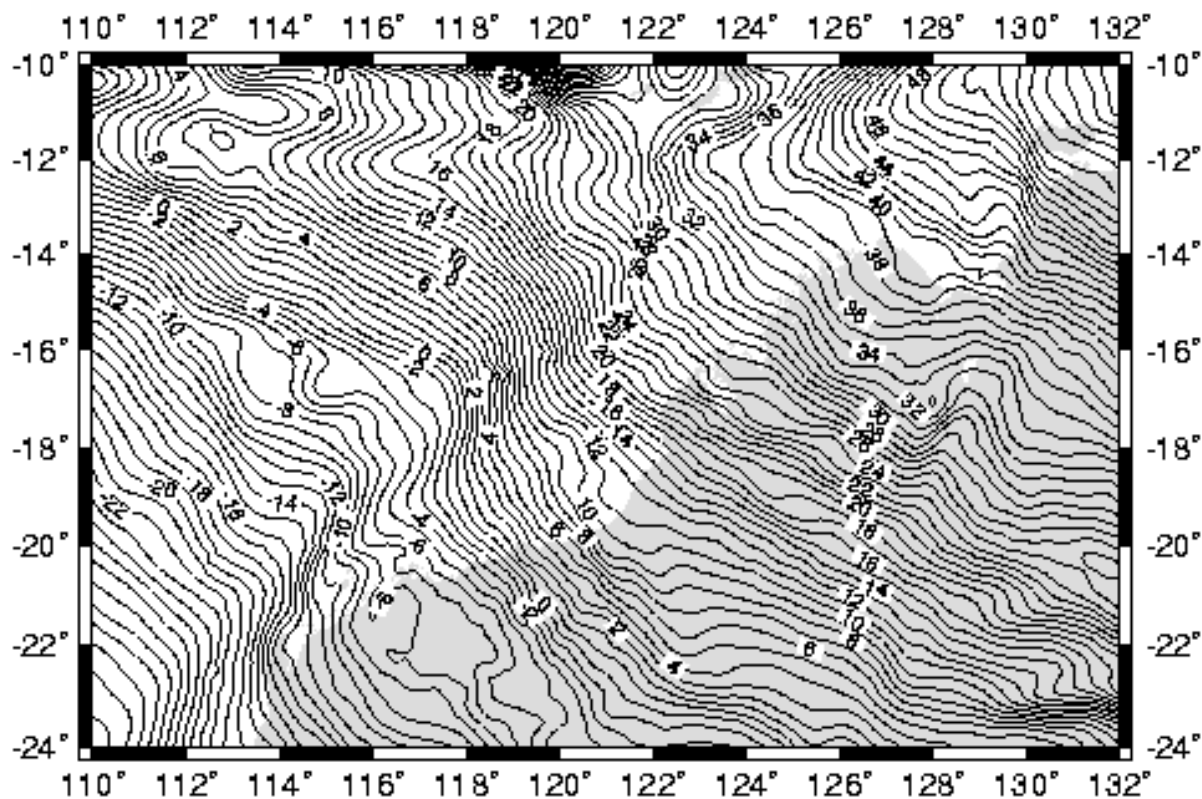


**Figure 1.** The geoid of the North-West Shelf from OSU91A to  $M_{max} = 360$  at sea and AUSGEOID93 on land. (Mercator projection from WGS84. Contours in metres relative to WGS84.)

Despite the dominance of this trend, a preliminary interpretation is possible from the geoidal anomalies in Figure 1. First, however, it is pertinent to describe how the geoid ‘reacts’ to sub-surface geological structures: An uplift in the geoid is generated by high density sub-surface features and *vice versa*. Therefore, it is reasonable to assume that relative geoid highs correspond to old, well-compacted and thus dense rocks, usually associated with continental massifs and shields. Conversely, relative geoidal lows indicate structures of lower mass density, such as sedimentary basins and large siliceous igneous intrusions. A simple analogy is that the mass excess

pulls the sea water towards it, thus uplifting the sea surface, and conversely for a mass deficit.

The contours of the geoid in Figure 1 can be correlated with known geological features, shown in Figure 2 of Australian Geological Survey Organisation North-West Shelf Study Group (1994). For example, an even geoid gradient, centred at 14°S, 117°E, coincides with the Argo Abyssal Plain, and a relative geoid high is co-located with the Precambrian rocks that make up the Pilbara Block. The Java Trench, the boundary of the Australian Plate and the Eurasian

Plate, is also clearly evident in the north of Figure 1 as a line approximately coincident with the 12°S parallel.

Bathymetric features are also delineated in the geoid in Figure 1. The edge of the continental shelf, which is commonly assumed to coincide with the 200 m depth contour, is a dominant feature which runs in a near-straight line from 24°S, 111°E to 10°S, 125°E. This illustrates yet another application of the marine geoid to mapping the edge of the continental shelf, without the need for expensive ship-based hydrographic surveys. Nevertheless, both the bathymetric and geological features are dominated by the regional geoid gradient, whose removal will be described next.

## SPECTRAL ANALYSIS OF THE GEOID AND GRAVITY ANOMALIES

There is an approximate relationship between the spectral content (information per wavelength) of the geoid and the depth of mass density anomaly which generates that particular geoid wavelength. However, the inherent non-uniqueness of geopotential field inversion should first be highlighted. Any number of configurations of various masses at different depths can produce the same geoid height. This is an important factor that must be taken into consideration when estimating sub-surface information from the geoid, or other potential field data.

Following the general procedure of Bowin (1983), the maximum depth ( $z$ ) at which a point mass anomaly ( $\delta m$ ) generates the geoid height at the surface of the Earth is given by

$$N = \frac{G\delta m}{z\gamma} \quad (4)$$

where  $G$  is the Newtonian gravitational constant and  $\gamma$  is normal gravity. This spherical formula is perfectly valid because a single point mass generates a gravitational potential field according to Newton's law

of gravitation. Bruns's formula (Heiskanen and Moritz, 1967, p. 85) was used to convert the gravitational potential to a geoid height in equation (4).

Similarly, the gravity anomaly corresponding to the same point mass is

$$\Delta g = \frac{G\delta m}{z^2} \quad (5)$$

Equations (4) and (5) are now combined to give the limiting depth at which a point mass can exist to create the observed geoid and gravity anomalies at the Earth's surface

$$z = \frac{\gamma N}{\Delta g} \quad (6)$$

Equation (6) is extended to the frequency domain by using the spectral relations in equations (1) and (3). These are inserted into equation (6) to yield an estimate of the maximum depth of causative mass anomaly, as a fraction of the Earth's radius ( $r$ ), which corresponds to each spherical harmonic degree ( $n$ )

$$z_n = \frac{r}{(n-1)} \quad (7)$$

Each spherical harmonic degree also corresponds to the wavelength ( $\lambda$ ) of geoid and gravity anomaly features at the Earth's surface

$$\lambda = \frac{360}{n} \quad (8)$$

where  $\lambda$  is in arc degrees. Therefore, equation (7) can be re-written as

$$z_n = \frac{r\lambda}{(360 - \lambda)} \quad (9)$$

For example, a geoidal feature of wavelength one arc degree at the Earth's surface (~110 km) is commensurate with spherical harmonic degree 360 and is assumed to correspond to mass anomalies

above a depth of ~18 km (ignoring non-uniqueness). In order to decrease this limiting depth, a higher resolution geoid is required.

Equations (7) and (9), respectively, imply that the low-degree or long-wavelength component of the geoid originates primarily from deep within the Earth and successively shorter wavelengths are added from increasingly shallower mass density anomalies. However, this argument is confounded by the problem of non-uniqueness. Some authors have suggested that all long-wavelength geoidal undulations can be adequately described by mass variations in the upper mantle and lithosphere (eg, Khan, 1977; Lambeck, 1988). Conversely, others such as Allan (1972) and Bowin (1983) have suggested that the wavelength of geopotential is purely depth-dependent, with longer wavelengths originating from greater depths. These differing conclusions seem to depend upon the approach taken and, at present, it cannot be proven which, if either, is more accurate. Therefore, the depths inferred from equations (7) and (9) will always be overestimates. However, it will be assumed in this study that the majority of long-wavelength geoidal undulations follow the relationship in equation (9).

In order to reveal these short-wavelength geoidal features, which are assumed to reflect crustal and lithospheric structures, the long-wavelength component of the geoid, assumed to originate in the mantle, is removed by a process termed detrending. The OSU91A geopotential model is evaluated to any arbitrary spherical harmonic degree  $L$  ( $<360$ ) using equation (1), then subtracted from the complete geoid solution to leave residual geoid anomalies

$$\delta N_{L+1} = N - N_L \quad , \quad (10)$$

where  $N_L$  is the partial expansion of OSU91A, which has been truncated at spherical harmonic degree  $L$ .

The wavelength of geoidal undulations removed by this detrending process is calculated using equation (8). This, in turn, corresponds to removing the effect of mass anomalies deeper than the limit given by equation (9). For example, detrending the geoid by  $L = 20$  removes wavelengths up to and including  $18^\circ$  (~1980 km) on the Earth's surface and yields residual geoid anomalies which exhibit the effects of density anomalies of less than ~335 km in depth. A higher degree of detrending removes progressively shorter wavelengths, corresponding to shallower mass density anomalies. This is essentially a process of high-pass filtering which allows a spectral study of the residual geoid in terms of Earth structure above a certain limiting depth.

## **A CASE STUDY: THE NORTH-WEST SHELF OF AUSTRALIA**

The ability of the residual geoid anomalies to define the lateral extent of tectonic elements is demonstrated and discussed for the specific example of the North-West Shelf of Australia. The OSU91A and AUSGEOID93 gravimetric geoids are detrended at varying degrees in order to estimate the limiting depths of major structural features in this region. The residual geoidal anomalies revealed by this progressive detrending are then correlated to the geologically well-known features given in Figure 2 of Australian Geological Survey Organisation North-West Shelf Study Group (1994).

Figures 2 and 3 show two particular examples of the residual geoid, one for  $L = 20$  and one for  $L = 60$ . However, there are 357 options for detrending the degree-360 OSU91A geoid model – these two examples are used specifically to illustrate the use of the geoid in geophysics.

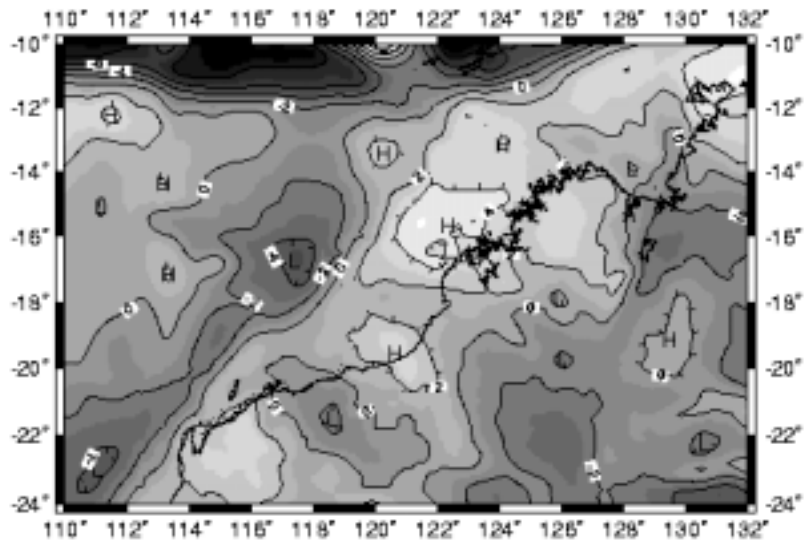


**Figure 2.** The  $L = 20$  residual geoid of the North-West Shelf ( $55 \text{ km} < \lambda < 1980 \text{ km}$ ;  $z < 335 \text{ km}$ ). (Mercator projection from WGS84. Grey-scale contours in metres.)

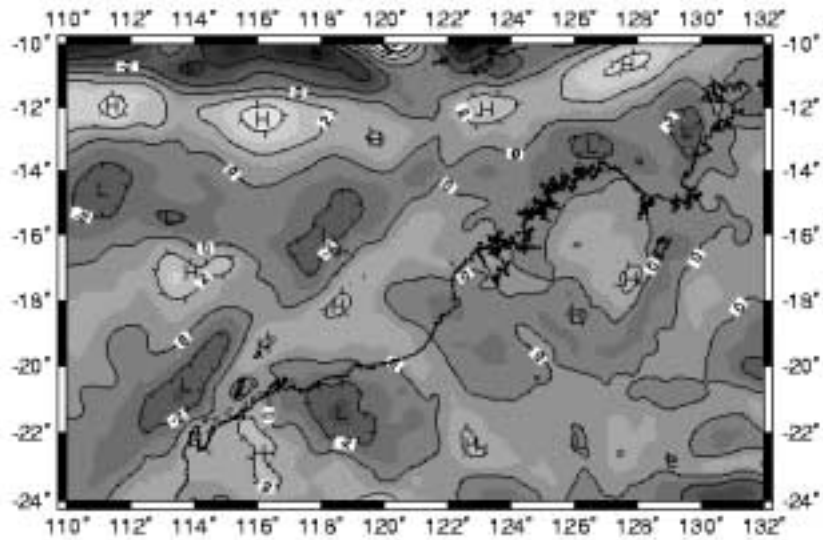


**Figure 3.** The  $L = 60$  residual geoid of the North-West Shelf ( $55 \text{ km} < \lambda < 660 \text{ km}$ ;  $z < 108 \text{ km}$ ). (Mercator projection from WGS84. Grey-scale contours in metres.)

Figure 2 ( $L = 20$ ) corresponds to geoid wavelengths between 1980 km and 55 km and limiting depths of less than 335 km. Figure 3 ( $L = 60$ ) corresponds to

wavelengths between 660 km and 55 km and limiting depths of less than 108 km. In both of these Figures, the edge of the Australian continental shelf ( $24^\circ\text{S}$ ,  $111^\circ\text{E}$  to  $10^\circ\text{S}$ ,  $125^\circ\text{E}$ ) and the boundary

between the Australian and Eurasian Plates ( $12^{\circ}\text{S}$  parallel) become more pronounced than in Figure 1. This is because the process of detrending has removed the long-wavelength, south-west to north-east geoidal gradient that obscured the more subtle features in Figure 1.

In Figure 2, the correlation between the residual geoid anomalies and the major tectonic units summarised in Figure 2 of Australian Geological Survey Organisation North-West Shelf Study Group (1994) become more evident. For instance, the following geological features can be clearly seen offshore Australia: the Argo Abyssal Plain (centred at  $14^{\circ}\text{S}$ ,  $117^{\circ}\text{E}$ ); the Carnarvon Basin (around  $20^{\circ}\text{S}$ ,  $114^{\circ}\text{E}$ ); the Kimberley Basin (centred at  $15^{\circ}\text{S}$ ,  $126^{\circ}\text{E}$ ); and the Bonaparte Basin (centred at  $14^{\circ}\text{S}$ ,  $129^{\circ}\text{E}$ ).

On land, the higher resolution of AUSGEOID93 allows clearer identification of geological features in Figure 2. Examples are: the Pilbara Block, intersected by the Hamersley Basin (centred at  $22^{\circ}\text{S}$ ,  $122^{\circ}\text{E}$ ); the Kidson Sub-basin (centred at  $23^{\circ}\text{S}$ ,  $126^{\circ}\text{E}$ ) within the Canning Basin; and the Victoria River Basin (centred at  $16^{\circ}\text{S}$ ,  $129^{\circ}\text{E}$ ) – and between the latter two basins is the Halls Creek Orogenic Belt. Many of these tectonic features cannot be generated solely by mass density anomalies at a depth of 335 km, as implied by equation (7). Therefore, the problem of non-uniqueness is exemplified where crustal and lithospheric structures effectively obscure the geoid signal generated by deeper Earth mass anomalies (cf. Lambeck, 1988).

In Figure 3, the Argo Abyssal Plain, the Carnarvon Basin, the Kimberley Basin, the Bonaparte Basin and the Hamersley Basin become more pronounced than in Figure 2. Of more interest is that features not previously discernible in the geoid now become clear in Figure 3. For example, the Browse Basin

(centred at  $14^{\circ}\text{S}$ ,  $124^{\circ}\text{E}$ ) and Canning Basin (around  $20^{\circ}\text{S}$ ,  $124^{\circ}\text{E}$ ) become evident. To the east of the Canning Basin the Leopold and Halls Creek Orogenic Belts are clearly visible.

Another point of interest is the elimination of some geoidal features when a higher degree of detrending is applied ( $L = 60$  as opposed to  $L = 20$  in this case). This suggests that these geoidal features are generated by mass anomalies at a depth greater than approximately 110 km. For example, the Kidson Sub-basin which forms the south-eastern part of the Canning Basin is not seen in Figure 3, whereas it was evident in Figure 2. The tectonic implications of this observation are beyond the scope of this discussion. (However, for those interested readers, files of residual geoid anomalies, detrended by different degrees, are available from the author.) Many other geological features can be delineated in Figures 2 and 3, although an exhaustive interpretation of the geoid of the North-West Shelf was not the objective of this paper. Instead, the geoid has been shown to provide information of the location of known tectonic structures.

## CONCLUSIONS

This paper has not set out to prove the geoid as a revolutionary new geophysical technique which supersedes all other approaches. Instead, the geoid offers an additional and complementary technique for use with other dependent or independent data to help the geoscientist determine the Earth's internal structure.

As the geoid has been shown to determine the lateral extent of known geological structures, it is reasonable to assume that it can be used to locate and map previously unknown structures. When the geoid is applied in the frequency domain, using

spherical harmonic analysis, features of increasingly subtle detail can be revealed by progressive stages of high-pass filtering. Although the geoid has been proven capable of delineating lateral features, it is relatively ineffective at constraining the depth of mass anomalies because of the inherent non-uniqueness of potential field inversion. Therefore, the geoid should not be relied upon too greatly in this three-dimensional respect unless independent data are available for constraint, such as seismic data.

## ACKNOWLEDGEMENTS

I would like to thank the following individuals and organisations: Professor Dick Rapp of the Ohio State University for providing the OSU91A model; Mr Jim Steed of the Australian Surveying and Land Information Group for providing the AUSGEOID93 model; and Dr R.A. Facer, Dr M.C. Dentith, Dr A. Trench, Miss A.K. Davies and Mrs K.J. Bessant for some useful comments on an earlier version of this paper.

## REFERENCES

- Allan, R.R., 1972, Depth sources of gravity anomalies: *Nature Physical Science* **236**, 22-23.
- Australian Geological Survey Organisation North West Shelf Study Group, 1994, Deep reflections on the North-West Shelf: changing perceptions of basin formation: pp. 63-76. In: Purcell P.G. and R.R., eds, *The sedimentary basins of Western Australia: Petroleum Exploration Society of Australia Symposium, Proceedings, Perth, 700pp.*
- Bowin, C.O., 1983, Depth of principal mass anomalies contributing to the Earth's geoidal undulations and gravity anomalies: *Marine Geodesy* **7**, 61-100.
- Chapman, M.E., 1979, Techniques for interpretation of geoid anomalies: *Journal of Geophysical Research* **84**, 3793-3801.
- Chase, C.G., 1985, The geological significance of the geoid: *Earth and Planetary Science Letters* **13**, 97-113.
- Christou, N.T., Vanicek, P. and Ware, C., 1989, Geoid and density anomalies: EOS: Transactions of the American Geophysical Union **70**, 625-631.
- Featherstone, W.E., 1992, A GPS controlled gravimetric determination of the geoid of the British Isles, D.Phil. thesis, Oxford University (unpublished).
- Hager, B., 1984, Subducted slabs and the geoid: constraints on mantle rheology and flow: *Journal of Geophysical Research* **89**, 6003-6015.
- Heiskanen, W.H. and Moritz, H., 1967, *Physical geodesy*: Freeman, San Francisco
- Kaula, W.M., 1967, Geophysical implications of satellite determinations of the Earth's gravitational field: *Space Science Review* **7**, 769-794.
- Khan, M.A., 1971, Some geophysical implications of the satellite-determined geogravity field: *Geophysical Journal of the Royal Astronomical Society* **23**, 15-43.
- Khan, M.A., 1977, Depth sources of gravity anomalies: *Geophysical Journal of the Royal Astronomical Society* **48**, 197-209.
- Lambeck, K., 1988, *Geophysical geodesy: the slow deformations of the Earth*: Oxford University Press, Oxford, England.
- Purcell, P.G. and Purcell, R.R., eds, 1988, *The North-West Shelf of Australia: Petroleum Exploration Society of Australia Symposium, Proceedings, Perth, 700pp.*
- Purcell, P.G. and R.R. Purcell (eds), 1994, *The sedimentary basins of Western Australia: Petroleum Exploration Society of Australia Symposium, Proceedings, Perth, 700pp.*
- Rapp, R.H., 1982, A Fortran program for the computation of gravimetric quantities from high degree spherical harmonic expansions: Report 334, Department of Geodetic Science and Surveying, Ohio State University, USA.
- Rapp, R.H., Wang, Y.M. and Pavlis, N.K., 1991, The Ohio State 1991 geopotential and sea surface topography harmonic coefficient models: Report 410, Department of Geodetic Science and Surveying, Ohio State University, USA.
- Rapp, R.H. and Wang, Y.M., 1993, Geoid undulation differences between geopotential models: *Surveys in Geophysics* **14**, 373-380.
- Runcorn, S.K., 1967, Flow in the mantle inferred from the low-degree harmonics of the geopotential: *Geophysical Journal of the Royal Astronomical Society* **14**, 375-384.
- Sandwell, D.T. and McAdoo, D.C., 1988, Marine gravity of the Southern Ocean and Antarctic margin from Geosat: *Journal of Geophysical Research* **93**, 10389-10396.

- Shum, C.K., Ries, J.C. and Tapley, B.D., 1995, The accuracy and applications of satellite altimetry: *Geophysical Journal International* **121**, 321-336.
- Stokes, G.G., 1849, On the variation of gravity on the surface of the Earth: Cambridge Philosophical Society, *Transactions* **8**, 672-695.
- Silver, P.G., Carlson, R.W. and Olson, P., 1988, Deep slabs, geochemical heterogeneity and the large scale structure of mantle convection: investigation of an enduring paradox: *Earth and Planetary Science Letters* **16**, 477-541.
- Steed, J. and Holtznagel, S., 1994, AHD heights from GPS using AUSGEOID93: *The Australian Surveyor* **39**, 295-305.
- Vanicek, P. and Christou, N.T., eds, 1994, *Geoid and its geophysical interpretations*: CRC Press, Florida.
- Zhang, K.F. and Featherstone, W.E., 1995, The statistical fit of high-degree geopotential models to the gravity field of Australia: *Geomatics Research Australasia* **63**, 1-18.